Single Molecule Emission Characteristics in Near-Field Microscopy

Randy X. Bian, Robert C. Dunn,* and X. Sunney Xie†
Pacific Northwest National Laboratory, P.O. Box 999, Richland, Washington 99352

P. T. Leung
Department of Physics, Portland State University, P.O. Box 751, Portland, Oregon 97207-0751
(Received 23 August 1995)

In near-field scanning optical microscopy (NSOM), the measured fluorescence lifetime of a single dye molecule can be shortened or lengthened, sensitively dependent on the relative position between the molecule and aluminum coated fiber tip. The modified lifetimes and other emission characteristics are simulated by solving Maxwell equations with the finite-difference time-domain (FDTD) method. The 2D computation reveals insight into the lifetime behaviors and provides guidance for nonperturbative spectroscopic measurements with NSOM. This new methodology is capable of predicting molecular emission properties in front of a metal/dielectric interface of arbitrary geometry.

PACS numbers: 78.47.+p, 07.79.Fc, 33.50.–j, 41.20.Jb

Recent advances in near-field scanning optical microscopy (NSOM) [1] make it possible to image the fluorescence from single molecules with nanometric resolution [2] and extend the single molecule spectroscopy work done at cryogenic temperature [3] to the room temperature regime. Single molecule fluorescence can be spectrally [4] and temporally resolved [5–7] with NSOM. In order to extract useful information from these experiments, however, perturbations to spectroscopic measurements induced by the aluminum coated fiber tip need to be characterized. In this paper, single molecule fluorescence lifetimes are experimentally determined and numerically computed as a function of the relative position of the molecule and the NSOM tip. In addition, spectral shifts and emission quantum yields are also computed. We present a new methodology that allows computation of the fluorescence characteristics for the specific NSOM tip geometry (or any arbitrary geometry). The computational results reveal significant insight into the experimental observations and allow us to predict the proper conditions under which spectroscopic measurements with NSOM can be performed with minimal perturbations.

Figure 1 shows a 4 μm×4 μm near-field fluorescence image of single sulforhodamine 101 molecules adsorbed on a silicate glass substrate. The image is obtained by raster scanning the sample with respect to the NSOM tip (Fig. 2) and collecting the fluorescence passing through the substrate [5]. The transition dipoles of the single molecules are determined to be parallel to, and randomly oriented on, the substrate surface [5]. The fluorescence decays of single molecules are measured by the time-correlated photon counting method [5–7]. Figure 3(a) shows three fluorescence decays of a molecule measured with the lateral displacements of $d = 0$, 30, and 60 nm at a constant tip-molecule gap of $h \sim 5$ nm. The lifetime

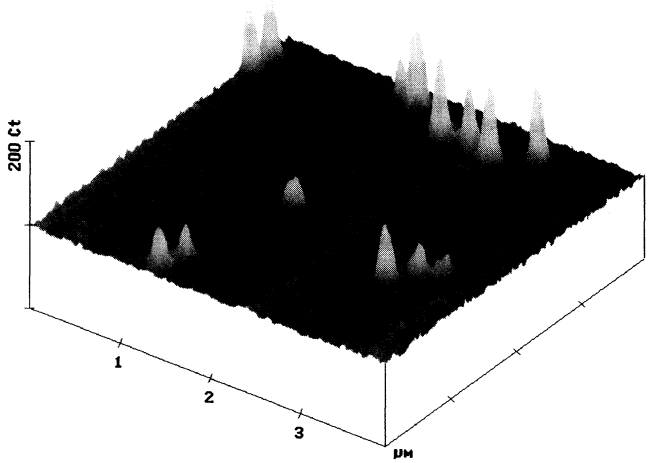

FIG. 1. Room temperature near-field fluorescence image (4 μm×4 μm) of single sulforhodamine 101 molecules adsorbed on a silicate glass substrate. Each peak (FWHM ~100 nm) in the image is due to a single molecule.

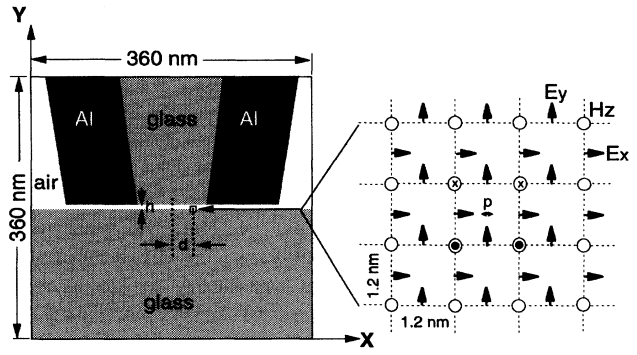

FIG. 2. Schematic of the NSOM tip with an aperture diameter of 96 nm. The FDTD domain is divided into a 300×300 grid of 1.2 nm square cells. The arrangements of the E_x, E_y, and H_z points are shown in the zoom-in inset. A horizontal point dipole is placed at the center of the cell with the four surrounding H_z points driven sinusoidally in the simulation. Molecular emission characteristics are evaluated as a function of the lateral displacement (d) and the tip-molecule gap (h).

 0031-9007/95/75(26)/4772(4)$06.00

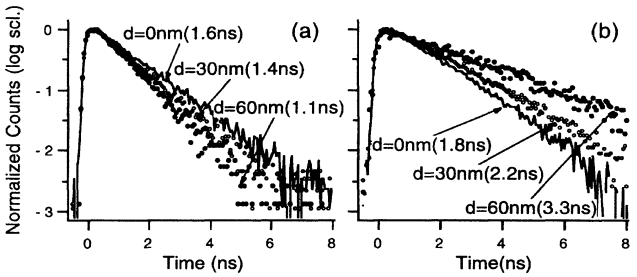

FIG. 3. Fluorescence decays of a single molecule measured at three lateral displacements from the tip center $d \sim 0$, 30, and 60 nm. At a tip-molecule gap $h \sim 5$ nm, the lifetime is the longest at the tip center and shortened at the tip edge. (b) The opposite trend in lifetime is seen at a larger tip-molecule gap of $h \sim 20$ nm. The lifetime measured in the far field without the NSOM tip is 2.7 ns.

is the longest when the tip is centered above the molecule and shortens as the tip is displaced laterally. This result has been previously reported and attributed to nonradiative energy transfer from the molecule to the aluminum coating of the NSOM tip [5,6]. Interestingly, however, an opposite trend in the lifetime has recently been observed by Trautman and Macklin [8] and confirmed by us for larger tip-molecule gaps. As shown in Fig. 3(b), with a tip-molecule gap of $h \sim 20$ nm, the lifetime is the shortest when the tip is centered above the molecule and lengthens when the tip is displaced laterally. In practice, due to the difficulty of obtaining nanometer-smooth aluminum coatings at the present time and consequently the uncertainties in controlling the actual tip-molecule gap with the shear force mechanism [9], measured lifetimes are extremely sensitive to tip morphology and often tip dependent. Theoretical understanding of the tip-molecule interactions are much needed to account for the observations.

A fluorescent molecule located a distance greater than nanometers away from a metal/dielectric interface can often be adequately treated as a damped-harmonic dipole driven by its own electric field reflected from the interface [10]:

$$\ddot{p} + \omega_0^2 p = (e^2/m)E_R - \gamma_0 \dot{p}\,, \tag{1}$$

where $p(t)$ is the oscillating dipole moment, γ_0 and ω_0 are the decay rate and emission frequency in the absence of the interface, respectively, and $E_R(t)$ is the electric field reflected from the interface projected onto the dipole direction. The e and m are the electronic charge and mass, respectively. In the presence of the metal/dielectric interface, both $p(t)$ and $E_R(t)$ oscillate with a slightly shifted frequency $(\omega_0 + \Delta\omega)$ and decay with a modified rate γ:

$$p(t) = p_0 \cos[(\omega_0 + \Delta\omega)t]e^{-\gamma t/2}, \tag{2}$$

$$E_R(t) = E_0 \cos[(\omega_0 + \Delta\omega)t - \phi]e^{-\gamma t/2}, \tag{3}$$

where p_0 and E_0 are the amplitudes of $p(t)$ and $E_R(t)$, with ϕ being the phase difference between the reflected field and the oscillating dipole. The modified decay rate γ and the frequency shift $\Delta\omega$ are solved by substituting Eqs. (2) and (3) into Eq. (1) and normalized to γ_0. In this phenomenological approach, the following expressions are obtained in SI units [11]:

$$\gamma/\gamma_0 = 1 + (6\pi q \varepsilon \varepsilon_0/p_0 k^3)E_0 \sin\phi\,, \tag{4}$$

$$\Delta\omega/\gamma_0 = -(3\pi q \varepsilon \varepsilon_0/p_0 k^3)E_0 \cos\phi\,, \tag{5}$$

where q is the intrinsic fluorescence quantum yield (in the absence of the metal/dielectric interface). ε is the dielectric constant of the medium (nonmetallic) surrounding the molecule, k is the propagation constant $(k = \omega_0\sqrt{\varepsilon}/c)$ in that medium, and ε_0 is the vacuum permittivity.

Hence the problem is reduced to a steady-state solution of classical electrodynamics, evaluating the amplitude (E_0) and the phase (ϕ) of the reflected field at the dipole position. Chance, Prock, and Silbey (CPS) have solved Eqs. (4) and (5) for infinitely extended flat interfaces [11]. For the specific geometry of the NSOM tip, in which the "edge effect" is expected to play an important role, one has to resort to numerical solutions for E_0 and ϕ.

Using the finite-difference time-domain (FDTD) method [12,13], we numerically integrate the Maxwell equations,

$$\nabla \times \vec{E} + \mu_0 \frac{\partial \vec{H}}{\partial t} = 0 \quad \text{and} \quad \nabla \times \vec{H} - \frac{\partial \vec{D}}{\partial t} = 0\,. \tag{6}$$

For dielectric regions, $\vec{D}(t) = \varepsilon\varepsilon_0\vec{E}(t)$, where $\varepsilon = 2.25$ for glass. For the aluminum regions, the frequency dependent complex susceptibility is given by the Drude model $\chi(\omega) = \omega_p^2/(\omega^2 + i\Gamma\omega)$, with $\omega_p = 15.565$ eV and $\Gamma = 0.608$ eV [14,15], respectively, and is accurate for $\omega > 1.5$ eV. We adopt the FDTD formulation of Leubbers, Hunsberger, and Kunz [14] to evaluate $\vec{D}(t)$:

$$\vec{D}(t) = \varepsilon_0\vec{E}(t) + \varepsilon_0 \int_0^t \vec{E}(t - \tau)\chi(\tau)\, d\tau\,, \tag{7}$$

where $\chi(\tau)$ is the Fourier transform of $\chi(\omega)$. The FDTD simulations were performed in two dimensions in order to reduce the computational time on an IBM RISC6000/590 computer. The 360 nm×360 nm area shown in Fig. 2 is divided into a 300×300 grid of 1.2 nm square cells. The arrangements of the H_z, E_x, and E_y points are shown in the zoom-in inset of Fig. 2 and the Mur absorbing boundary condition [16] is applied.

Similar FDTD approaches have been used to simulate the fields exiting NSOM tips [17]. However, here we need to mimic the radiation from a point dipole in FDTD. As shown in the inset of Fig. 2, a horizontal point dipole is placed at the center of a cell. The initial condition is set by sinusoidally driving the H_z at the four nodes of the cell enclosing the dipole: $H_z^n(i,j) \leftarrow \pm\sin(n\omega\Delta t) + H_z^n(i,j)$, where i, j are the cell indexes and n is the time step

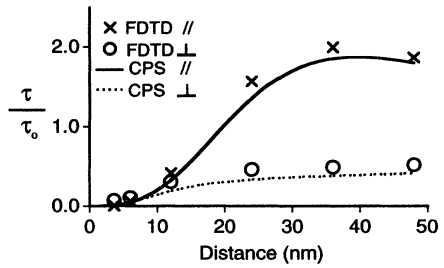

FIG. 4. Comparison of FDTD results with the CPS analytical solutions for the normalized lifetime τ/τ_0 of both a parallel and perpendicular dipole as a function of distance away from a flat aluminum surface.

index. At these four nodes, for each time step, a new value of $H_z^n(i,j)$ is calculated using the Yee algorithm [12], then summed with the driving source $\pm\sin(n\omega\Delta t)$ before being stored in the memory [13]. The H_z at the upper two nodes are taken 180° out of phase with respect to those at the lower two nodes. The H_z amplitudes at the four nodes are proportional to the dipole moment p_0. The driving frequency is 5×10^{14} Hz (600 nm emission wavelength) and Δt is one-thousandth of an optical cycle. Steady-state solutions are reached in three optical cycles.

The reflected field $E_R(t)$ is obtained by taking the average of the two closest E_x points to the horizontal dipole in the Fig. 2 inset (the two closest E_y points are used for a vertical dipole). $E_R(t) = E_{\text{tip}}(t) - E_{\text{free}}(t)$, where $E_{\text{tip}}(t)$ and $E_{\text{free}}(t)$ are the time series in the presence and absence of the NSOM tip and substrate, respectively. The amplitude E_0 and phase ϕ are obtained from $E_R(t)$ by fast Fourier transform [14].

As a necessary check of our methodology, a comparison is made in Fig. 4 between the FDTD results and the CPS analytical solutions for normalized fluorescence lifetimes ($\tau/\tau_0 = \gamma_0/\gamma$) of both a parallel and a perpendicular dipole in front of a flat aluminum surface. The good agreement between the two results confirms the validity of the 2D FDTD scheme.

The left column of Fig. 5 shows the FDTD results for a horizontal dipole. In Figs. 5(a) and 5(b), E_0 and ϕ are plotted as a function of the lateral displacement d for two different tip-molecule gaps ($h = 6$ and 24 nm). With the assumption of an intrinsic quantum yield $q = 1$, τ/τ_0 is plotted in Fig. 5(c). It is clear from Fig. 5(c) that the lifetime is a very sensitive function of the lateral displacement due to the influence from both E_0 and ϕ. Interestingly the computed results clearly show the reversal in lifetime behavior in going from small to large tip-molecule gaps, entirely consistent with the experimental observations.

In order to gain a physical insight into the computed lifetimes, we separate the contributions from the radiative rate (γ_r) and the nonradiative rate ($\gamma_{\text{nr}} = \gamma - \gamma_r$). In our FDTD computation, the Poynting vector $\vec{S} = \vec{E} \times \vec{H}$ is cycle averaged after reaching a steady state. Integrating the cycle averaged $\vec{S}$ over a closed boundary enclosing the molecule and the tip results in the steady-state value for the total radiated power (W) to the far field. From this a normalized radiative rate is obtained as $\gamma_r/\gamma_0 = W_{\text{tip}}/W_{\text{free}}$, where W_{tip} and W_{free} denote the total radiation powers in the presence and absence of the tip, respectively. It follows that the apparent emission quantum yield ($q' = \gamma_r/\gamma$) gives the fraction of energy released by the molecule as radiation going to the far field.

In Figs. 5(d)–5(f) γ_r/γ_0, $\gamma_{\text{nr}}/\gamma_0$, and q' are shown for the horizontal dipole. Interestingly, at a small tip-molecule gap, q' is significantly reduced at the tip edges due to the increased nonradiative energy transfer rate (γ_{nr}). On the other hand, for the larger gap, the

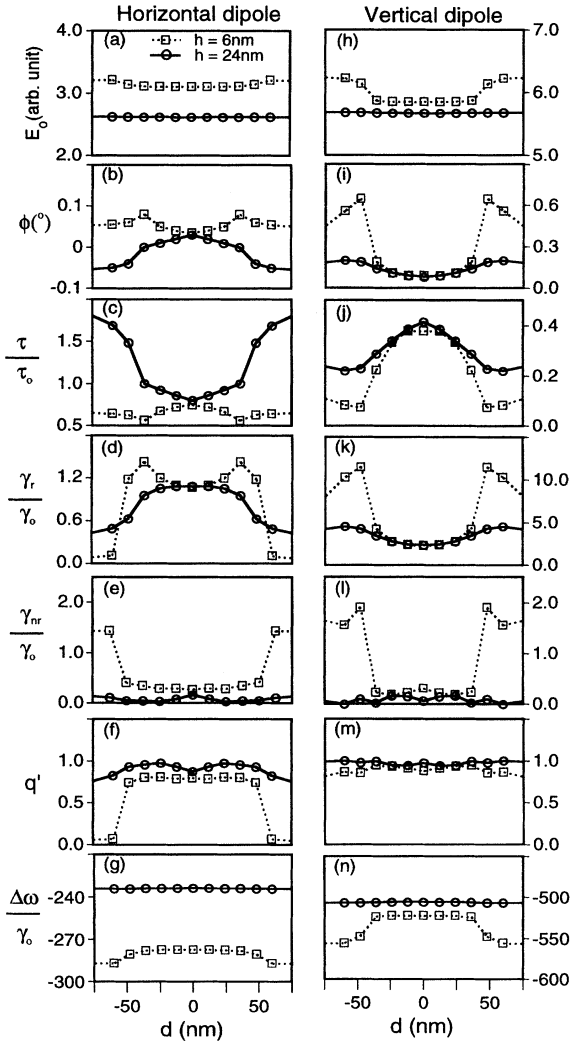

FIG. 5. FDTD results for both a horizontal dipole [left column, (a)–(g)] and a vertical dipole [right column, (h)–(n)] as a function of the lateral displacement d evaluated at tip-molecule gaps $h = 6$ and 24 nm. From top to bottom, the quantities simulated are the reflected field amplitude E_0 and phase ϕ, normalized lifetime τ/τ_0, normalized radiative rate γ_r/γ_0 and nonradiative rate $\gamma_{\text{nr}}/\gamma_0$, apparent quantum yield q', and spectral shift $\Delta\omega/\gamma_0$.

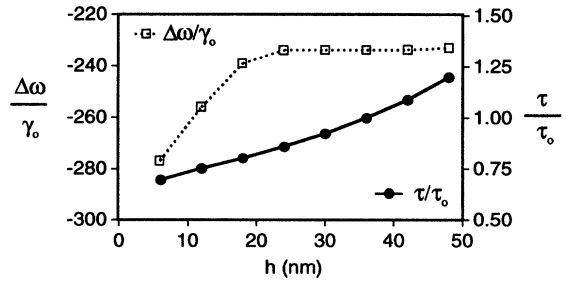

FIG. 6. FDTD results for normalized lifetime τ/τ_0 and spectral shift $\Delta\omega/\gamma_0$ as a function of tip-molecule gap h for a horizontal dipole centered at the NSOM tip.

fluorescence decay is dominated by the radiative rate ($\gamma_r > \gamma_{nr}$), which is reduced at the tip edges (opposite of γ_{nr}). As a result, q' remains close to unity across the tip. These results clearly demonstrate that the origin for the reversal in lifetime behaviors observed at different tip-molecule gaps results from the competition between radiative and nonradiative mechanisms.

Fig. 5(g) shows the spectral shift $\Delta\omega/\gamma_0$ [Eq. (5)] for the horizontal dipole. For a typical dye molecule with $\gamma_0 \sim 3 \times 10^8$ s^{-1}, the frequency is redshifted by $(1.1-1.4) \times 10^{10}$ Hz. At room temperature, this shift is negligible compared to the broad single molecule spectral width [4]. For high frequency resolution NSOM experiments done at cryogenic temperatures [18], however, the position dependent frequency shifts predicted in Fig. 5(g) can be significant [19]. Figure 6 shows the variation of $\Delta\omega/\gamma_0$ and τ/τ_0 as a function of h for a centered horizontal dipole ($d = 0$).

Finally, the right column of Fig. 5 [(h)–(n)] shows the FDTD results for E_0, ϕ, τ/τ_0, γ_r/γ_0, γ_{nr}/γ_0, q', and $\Delta\omega/\gamma_0$ of a vertical dipole. While the nonradiative (γ_{nr}) rate has a similar behavior to that of the horizontal dipole, fluorescence decays are dominated by the magnitude of the radiative rates (γ_r). Therefore the apparent quantum yield (q') is close to unity across the tip.

It is important to note that all the FDTD results for τ/τ_0, γ_r/γ_0, γ_{nr}/γ_0, q', and $\Delta\omega/\gamma_0$ are independent of the dipole strength; thus they are not only applicable to single molecule experiments but also to experiments on molecular aggregates [20] and semiconductor systems [21] as long as the point dipole approximation still holds. While the 2D results reveal the physical mechanism, a more quantitative agreement with experiments requires a 3D computation and smoother aluminum coatings. We are currently working on both aspects and modeling the effects of coating morphology with the FDTD approach.

The characterization of the tip-molecule interactions provides guidance for obtaining unperturbed spectroscopic information, even with the less-than perfect NSOM tips currently available. Our results indicate that perturbations to room temperature excitation and emission spectra are negligible. While the nonradiative energy transfer can be minimized with larger tip-molecule gaps and by centering the tip above the molecule [5], a perturbation to the radiative rate can hardly be avoided. However, for many other intrinsically fast dynamical processes, such as photoinduced electron transfer reactions or exciton dynamics, population lifetimes can be measured essentially free from perturbation. [This is evident from Eq. (4), when the intrinsic quantum yield q is much less than one, then $\gamma/\gamma_0 \sim 1$.] The collection of unperturbed spectral and temporal information at the nanometric dimension with single molecule sensitivity opens up many exciting possibilities in a variety of disciplines.

We thank Jay Trautman of AT&T Bell Labs for communicating and discussing results with us. This research was supported by the U.S. Department of Energy (DOE). Pacific Northwest National Laboratory is operated by Battelle Memorial Institute for DOE under Contract No. DE-AC06-76L0 1830.

*Present address: Department of Chemistry, University of Kansas, Lawrence, KS 66045.
†To whom correspondence should be addressed.

[1] For a review, see E. Betzig and J. K. Trautman, Science **257**, 189 (1992).
[2] E. Betzig and R. J. Chichester, Science **262**, 1422 (1993).
[3] For a review, see W. E. Moerner, Science **265**, 46 (1994).
[4] J. K. Trautman *et al.*, Nature (London) **369**, 40 (1994).
[5] X. S. Xie and R. C. Dunn, Science **265**, 361 (1994).
[6] W. P. Ambrose *et al.*, Science **265**, 364 (1994).
[7] R. C. Dunn *et al.*, J. Phys. Chem. **98**, 3094 (1994).
[8] J. K. Trautman and J. J. Macklin, Chem. Phys. (to be published).
[9] E. Betzig, P. L. Finn, and J. S. Weiner, Appl. Phys. Lett. **60**, 2484 (1992); R. Toledo-Crow *et al.*, Appl. Phys. Lett. **60**, 2957 (1992).
[10] H. Kunh, J. Chem. Phys. **53**, 101 (1970).
[11] R. R. Chance, A. Prock, and R. Silbey, Adv. Chem. Phys. **37**, 1 (1978).
[12] K. S. Yee, IEEE Trans. Antennas Propag. **14**, 302 (1966).
[13] A. Teflove and M. E. Brodwin, IEEE Trans. Microwave Theory Tech. **23**, 623 (1975).
[14] R. J. Luebbers, F. Hunsberger, and K. S. Kunz, IEEE Trans. Antenna Propag. **39**, 29 (1991).
[15] The ω_p and Γ values are derived from L. Novotny and C. Hafner, Phys. Rev. E **50**, 4094 (1994).
[16] G. Mur, IEEE Trans. Electromagn. Compat. **23**, 377 (1981).
[17] D. A. Christensen, Ultramicroscopy **57**, 189 (1995); J. Kann *et al.*, J. Opt. Soc. Am. A **12**, 501 (1995).
[18] W. E. Moerner *et al.*, Phys. Rev. Lett. **73**, 2764 (1994); E. Betzig, Opt. Lett. **20**, 237 (1995).
[19] The room temperature dielectric constant of aluminum used in FDTD modeling is close to the value at 4 K. See *Handbook of Optical Constants of Solids,* edited by E. D. Palik (Academic Press, New York, 1985), Vol. 1, p. 394.
[20] D. A. Higgins and P. F. Barbara, J. Phys. Chem. **99**, 3 (1995); D. Birnbaum, S. Kook, and R. Kopelman, J. Phys. Chem. **97**, 3091 (1993).
[21] H. F. Hess *et al.*, Science **264**, 1740 (1994).

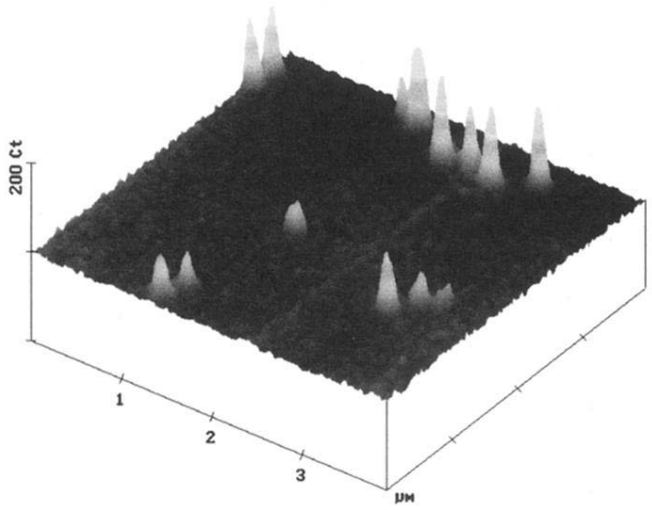

FIG. 1. Room temperature near-field fluorescence image (4 μm$\times$4 μm) of single sulforhodamine 101 molecules adsorbed on a silicate glass substrate. Each peak (FWHM $\sim$100 nm) in the image is due to a single molecule.